GIACOVAZZO, C. (1977*c*). *Acta Cryst.* A**33**, 539–547.
GIACOVAZZO, C. (1978). *Acta Cryst.* A**34**, 562–574.
GIACOVAZZO, C. (1979). *Acta Cryst.* A**35**, 296–305.
GIACOVAZZO, C. (1980*a*). *Direct Methods in Crystallography*. London: Academic Press.
GIACOVAZZO, C. (1980*b*). *Acta Cryst.* A**36**, 74–82.
GIACOVAZZO, C. (1980*c*). *Acta Cryst.* A**36**, 362–372.
GIACOVAZZO, C., SPAGNA, R., VICKOVIĆ, I. & VITERBO, D. (1979). *Acta Cryst.* A**35**, 401–412.
GREEN, E. A. & HAUPTMAN, H. (1978). *Acta Cryst.* A**34**, 216–223.
HAUPTMAN, H. & GREEN, E. A. (1978). *Acta Cryst.* A**34**, 224–229.
JAMES, V. J. & STEVENS, J. D. (1977). *Cryst. Struct. Commun.* **6**, 241–246.
KARLE, I. L., KARLE, J. & ESTLIN, J. A. (1967). *Acta Cryst.* **23**, 494–500.
KLUG, A. (1958). *Acta Cryst.* **11**, 515–543.

Acta Cryst. (1980). A**36**, 1025–1030

Measurement of X-ray *Pendellösung* Intensity Beats in Diffracted White Radiation from Silicon Wafers

BY T. TAKAMA, M. IWASAKI AND S. SATO

Department of Applied Physics, Faculty of Engineering, Hokkaido University, Sapporo, 060, Japan

(*Received* 21 *March* 1980; *accepted* 8 *July* 1980)

Abstract

Pendellösung intensity beats of white radiation diffracted from parallel-sided single-crystal wafers of silicon were measured by a solid-state detector. After a few corrections, the extremum positions in the beat were measured to evaluate the atomic scattering factors for various reflections. The scattering factor shows a dependence on wavelength, λ, which can be interpreted by the anomalous dispersion term, f', as calculated by Cromer [*Acta Cryst.* (1965), **18**, 17–23]. The obtained values of the atomic scattering factor expressed as linear functions of wavelength are listed with those at $\lambda = 0{\cdot}5594$ Å for comparison with the data so far obtained with Ag $K\alpha_1$ and wedge crystals. The values for 111 and 220 reflections in the present experiment, 10·59 and 8·40, were almost the same as Tanemura & Kato's [*Acta Cryst.* (1972), A**28**, 69–80], $10{\cdot}66_4$ and $8{\cdot}46_3$, respectively.

1. Introduction

A striking example of the dynamical diffraction effect of X-rays is the *Pendellösung* fringe appearing in the topographic image of perfect wedge crystals. Kato & Lang (1959) first observed the fringes for silicon and quartz using characteristic radiation. The fringes are produced by the interaction between two wave fields with slightly different wave vectors in the crystal, and the fringe spacing can be expressed as a function of the structure factor of the crystal. Many workers have measured the fringe spacing in topographs for the purpose of obtaining the structure factors of silicon (Hattori, Kuriyama, Katagawa & Kato, 1965; Hart, 1966; Hart & Milne, 1969; Tanemura & Kato, 1972), germanium (Batterman & Patel, 1968; Persson, Zielińska-Rohozińska & Gerward, 1970) and others (Yamamoto, Homma & Kato, 1968; Yasuda, Hondoh & Higashi, 1979). This method requires accurate collimation of characteristic X-rays and precise shaping of the wedge specimen.

The *Pendellösung* fringes have also been observed in the topographic images of white radiation (Hashimoto, 1965; Kozaki, Ohkawa & Hashimoto, 1968; Aristov, Shmytko & Shulakov, 1977*a*,*b*). These fringes are apparently produced by the change in extinction distance with the wavelength of diffracted X-rays. Aristov *et al.* (1977*a*,*b*) tried to measure the atomic scattering factors of silicon and germanium using white X-ray topographs from parallel-sided and wedge-shaped specimens. It seems rather difficult in this case to determine the accurate value of the wavelength corresponding to the position on the topographic film.

In the present experiment an attempt is made to measure the *Pendellösung* intensity beat of white radiation directly with a solid-state detector. X-ray intensities in *hkl* Laue spots from silicon single-crystal wafers are successively measured at different Bragg angles. One observes the clear *Pendellösung* intensity beat following the variation in wavelength. The values of the atomic scattering factor of silicon are obtained with their wavelength dependence for various reflections by measuring the extremum positions in the intensity beats. Measured values and their wavelength dependence are discussed and compared with the previous data from topographic methods (Hattori *et al.*,

0567-7394/80/061025-06$01.00

1965; Tanemura & Kato, 1972) and with the theoretical calculation by Cromer (1965).

2. Experimental procedure

White radiation from a tungsten tube falls on the specimen through a slit system consisting of a Soller slit and a cylindrical collimator as shown in Fig. 1. The Soller slit limits the horizontal beam divergence to within 0·1° and the cylindrical collimator produces a narrow beam of about 1 mm in diameter. A single-crystal goniometer head is set on the specimen stage of a diffractometer which rotates through an angle θ while the X-ray source on the arm rotates through 2θ around the diffractometer axis. A solid-state detector of intrinsic Ge with a cooling vessel is placed where the beam from the source at $2\theta = 0°$ enters the detector directly through the center of the diffractometer.

Wafers with parallel-sided planes of {110} and {111} were cut from silicon single crystals grown by the floating-zone technique. The cut wafers were mechanically polished and then etched in a solution of 1 part HF and 1 part HNO_3 to remove the damaged surface layers. A topographic examination revealed that the wafers were free from dislocations. Several specimens with different thicknesses were prepared (Table 1), the thickness being measured by a micrometer with an accuracy of about 1 μm. Specimens having a {110}

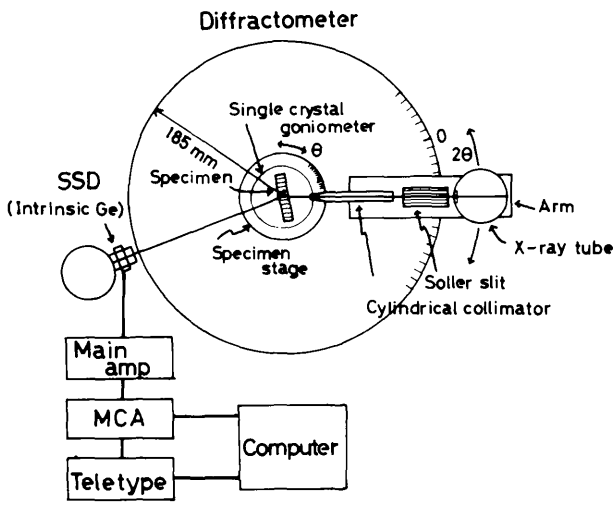

Fig. 1. Schematic diagram showing the experimental arrangement.

Table 1. *Atomic scattering factors obtained in the present experiment*

Values are represented as linear functions of λ. Special values at $\lambda = 0{\cdot}5594$ Å are also listed in comparison with the values reported so far. An asterisk indicates statistical probable error.

				Atomic scattering factor $f_{hkl} = (f^0_{hkl} + f')\,e^{-M}$				
				White radiation (present work)			Characteristic radiation	
hkl	Specimen no.	Thickness (mm)	Surface		At $\lambda = 0{\cdot}5594$ Å (Ag $K\alpha_1$)	Averaged value	Hattori *et al.* (1965) Mo $K\alpha_1$ and Ag $K\alpha_1$	Tanemura & Kato (1972) (Ag $K\alpha_1$)
111	1	0·195	{110}	$(10{\cdot}50 \pm 0{\cdot}01^*) + (0{\cdot}19 \pm 0{\cdot}04^*)\lambda$	$10{\cdot}62 \pm 0{\cdot}01^*$	10·59	10·98	$10{\cdot}66_4$
	3	0·249	{110}	$(10{\cdot}46 \pm 0{\cdot}01) + (0{\cdot}15 \pm 0{\cdot}04)\lambda$	$10{\cdot}55 \pm 0{\cdot}02$			
220	1	0·195	{110}	$(8{\cdot}34 \pm 0{\cdot}01) + (0{\cdot}15 \pm 0{\cdot}04)\lambda$	$8{\cdot}43 \pm 0{\cdot}02$			
	2	0·245	{111}	$(8{\cdot}29 \pm 0{\cdot}02) + (0{\cdot}15 \pm 0{\cdot}06)\lambda$	$8{\cdot}38 \pm 0{\cdot}03$			
	3	0·249	{110}	$(8{\cdot}32 \pm 0{\cdot}01) + (0{\cdot}14 \pm 0{\cdot}05)\lambda$	$8{\cdot}40 \pm 0{\cdot}02$	8·40 ±0·02	8·58	$8{\cdot}46_3$
	4	0·289	{111}	$(8{\cdot}27 \pm 0{\cdot}01) + (0{\cdot}16 \pm 0{\cdot}04)\lambda$	$8{\cdot}37 \pm 0{\cdot}02$			
	5	0·345	{111}	$(8{\cdot}32 \pm 0{\cdot}01) + (0{\cdot}14 \pm 0{\cdot}06)\lambda$	$8{\cdot}40 \pm 0{\cdot}02$			
311	3	0·249	{110}	$(7{\cdot}60 \pm 0{\cdot}02) + (0{\cdot}17 \pm 0{\cdot}15)\lambda$	$7{\cdot}71 \pm 0{\cdot}03$	7·68	7·78	
	6	0·360	{110}	$(7{\cdot}54 \pm 0{\cdot}02) + (0{\cdot}18 \pm 0{\cdot}09)\lambda$	$7{\cdot}65 \pm 0{\cdot}02$			
400	1	0·195	{110}	$(6{\cdot}97 \pm 0{\cdot}01) + (0{\cdot}13 \pm 0{\cdot}09)\lambda$	$7{\cdot}05 \pm 0{\cdot}02$	7·04	7·02	
	3	0·249	{110}	$(6{\cdot}91 \pm 0{\cdot}02) + (0{\cdot}18 \pm 0{\cdot}07)\lambda$	$7{\cdot}02 \pm 0{\cdot}03$			
331	3	0·249	{110}	$(6{\cdot}77 \pm 0{\cdot}02) + (0{\cdot}05 \pm 0{\cdot}12)\lambda$	$6{\cdot}80 \pm 0{\cdot}03$	6·80	6·89	
422	3	0·249	{110}	$(6{\cdot}05 \pm 0{\cdot}02) + (0{\cdot}13 \pm 0{\cdot}10)\lambda$	$6{\cdot}13 \pm 0{\cdot}04$	6·13	6·20	

surface (nos. 1, 3, 6) were used to get 111, 220, 311, 400, 331 and 422 reflections and those having a {111} surface (nos. 2, 4, 5) the 220 reflection.

The specimen was mounted on the specimen stage so as always to keep the symmetrical Laue position during the θ–2θ rotation. The diffracted X-ray photons at a θ–2θ position were energy-analyzed by the SSD (solid-state detector)–MCA(multichannel pulse-height analyzer) system as shown in Fig. 2. The value of photon energy which corresponds to the channel number of the MCA was calibrated by using various γ-rays and X-ray emission lines of several elements. The area of the *hkl* peak, J_{hkl}, was integrated after subtracting the background intensity from the measured intensity distribution. The variation of J_{hkl} with respect to the photon energy or wavelength λ was obtained by repeating the same measurement at different θ–2θ positions for a fixed time interval during which the voltage applied (50 kV) and current through the X-ray tube (16 mA) were kept constant.

The intensity spectrum of incident white radiation, $I_0(E)$, was determined by measuring dynamically diffracted intensities of the 220 reflection from a thick silicon single crystal in the symmetrical Bragg case. The radiation was assumed to be unpolarized. The intensity equation of DeMarco & Weiss (1965) was utilized to get $I_0(E)$ by substituting the value of the atomic scattering factor $f_{220} = 8{\cdot}58$ (Hattori *et al.*, 1965). The Hönl formula (James, 1967) for the anomalous dispersion and the Victoreen equation (*International Tables for X-ray Crystallography*, 1962) for the mass absorption coefficient were also applied to evaluate $I_0(E)$.

3. Experimental results

Fig. 3 shows an example of the *Pendellösung* beat in integrated intensities for the 220 reflection obtained from specimen 2 with a thickness of 0·245 mm at 293 K. Each dot corresponds to the measured J_{hkl} for one θ–2θ setting, *i.e.* for a particular wavelength of X-rays. The spectrum of incident radiation, $I_0(E)$, obtained by the procedure described in § 2 is represented in Fig. 4. Having corrected J_{hkl} for $I_0(E)$, one obtains the true variation in integrated intensity with respect to the wavelength of X-rays as shown by the dots in Fig. 5.

According to the dynamical theory of X-ray diffraction with absorption, the diffracted intensity in the symmetrical Laue case, J_{hkl}, can be expressed, assuming unpolarized incident radiation, as follows (Kato, 1955; DeMarco & Weiss, 1965; Buras, Olsen, Gerward, Selsmark & Lindegaard Andersen, 1975):

$$J_{hkl} = K\, I_0(E)\, |F'_{hkl}|\, (R_{hkl,n} + |\cos 2\theta|\, R_{hkl,p})/2 \sin\theta, \quad (1)$$

where

$$R_{hkl,n,p} = \frac{\pi}{2} \exp(-\mu(E)t/\cos\theta) \left[\int_0^{2A_{n,p}} J_0(x)\, dx + J_0(2i|k|A_{n,p}) - 1 \right], \quad (2)$$

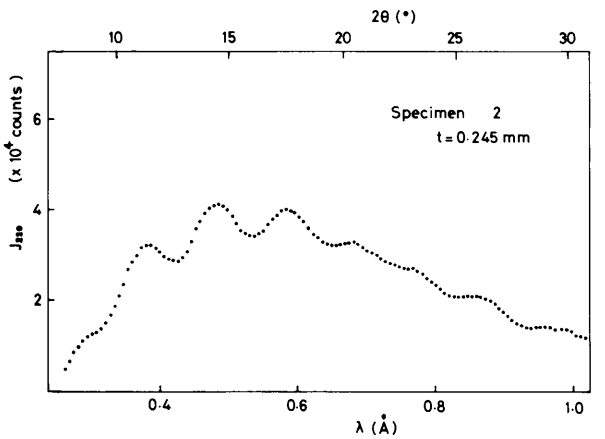

Fig. 3. *Pendellösung* beat in diffracted intensity of the 220 reflection, J_{220}. No corrections have been made.

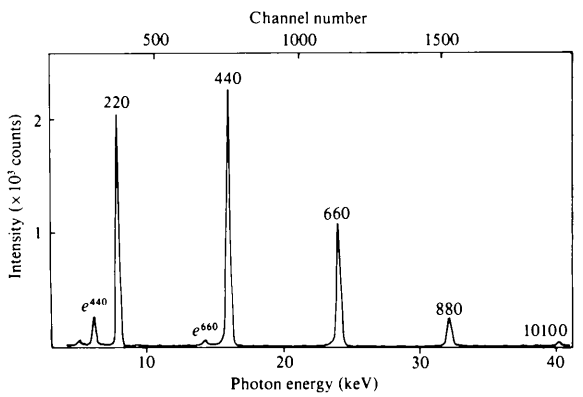

Fig. 2. Intensity spectrum of a Laue spot. Specimen: Si wafer, symmetrical Laue setting, *hh*0 reflection, $2\theta = 47°$; X-rays: 50 kV, 16 mA; time interval: 1000 s; e^{hh0}: escape peak.

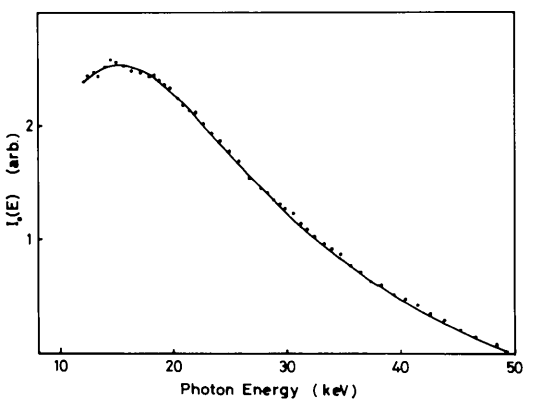

Fig. 4. Intensity spectrum of incident X-rays, $I_0(E)$. Dynamically diffracted intensities from a thick Si single crystal were utilized with the theory by DeMarco & Weiss (1965) in the symmetrical Bragg case. X-rays: 50 kV, 16 mA.

$$A_{n,p} = (e^2/mc^2)(\lambda t/\cos\theta)|F'_{hkl}|e^{-M}(C_{n,p}/V) \qquad (3)$$

and K = a constant depending on the experimental conditions; θ = Bragg angle; t = thickness of specimen; $\mu(E)$ = linear absorption coefficient; E = photon energy; J_0 = Bessel function of zeroth order; e^2/mc^2 = classical electron radius; V = volume of unit cell; $C_{n,p}$ = polarization factor, n,p = normal and parallel components, $C_n = 1$, $C_p = |\cos 2\theta|$; $F_{hkl} = F'_{hkl} + iF''_{hkl} = \sum_j (f^0_{hkl} + f' + if'')\exp 2\pi i\,\mathbf{H}_{hkl}\,\mathbf{r}_j$ = structure factor; $|k| = |F''_{hkl}/F'_{hkl}|$; e^{-M} = temperature factor.

The integral of the Bessel function in (2) oscillates with $A_{n,p}$, *i.e.* with $\lambda/\cos\theta$ when t is constant and the observed beat in J_{hkl} in Fig. 3 corresponds to this oscillation. In order to make the intensity beat clearer, the observed J_{hkl} was corrected for absorption and geometrical factors as shown in Fig. 6. The extremum positions were then determined by the least-squares method by assuming the parabolic intensity change near the extremum positions.

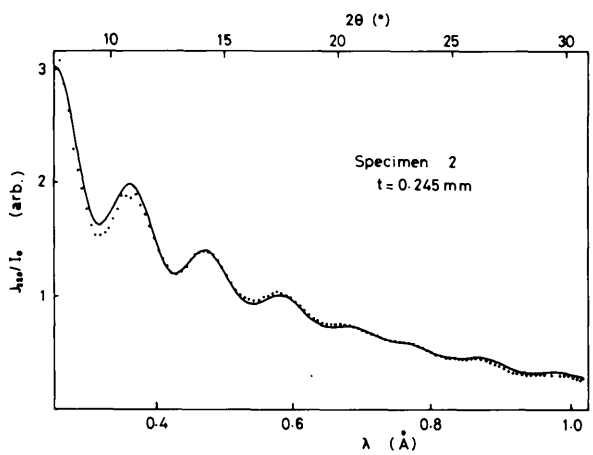

Fig. 5. Variation in J_{220}/I_0 with wavelength λ or Bragg angle 2θ. Dots: measured; Solid line: calculated with $f_{220} = 8{\cdot}29 + 0{\cdot}15\lambda$.

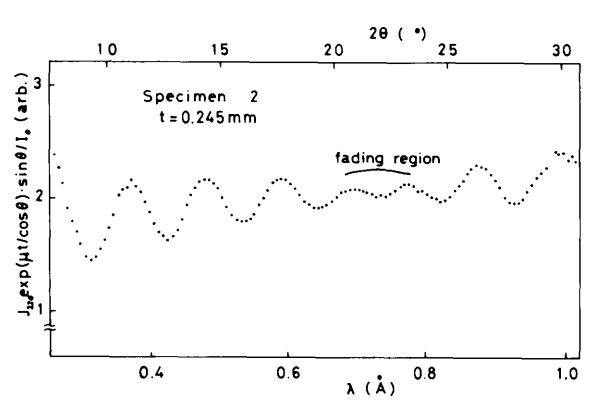

Fig. 6. *Pendellösung* beat in the 220 reflection. The corrections for incident spectrum, absorption factor and geometrical factor have been made. A fading region can be seen clearly.

Fig. 7 shows a diagram relating $|F'_{220}|e^{-M}t$ with λ or 2θ on which the calculated extremum positions are drawn. No effect of the modified Bessel function $J_0(2i|k|A_{n,p})$ in (2) on the peak position has been considered. The observed extremum positions in Fig. 6 are plotted on the diagram as shown by ×. Since we know the thickness of the specimen, the structure factor can be determined with its wavelength dependence in this figure. One sees a slight but clear increase in $|F'_{220}|e^{-M}t$ with λ at the observed extremum positions in Fig. 7.

The obtained atomic scattering factors, $f_{220} = (f^0_{220} + f')e^{-M}$ for five different specimens with different thicknesses are plotted together in Fig. 8. Even though the measured points scatter to some extent, it can be said that all the f_{220} values increase with the wavelength in the measured range. Similar dependence was also observed for other reflections as shown in Fig. 9. Since f^0_{hkl} is independent of λ for each reflection, the observed

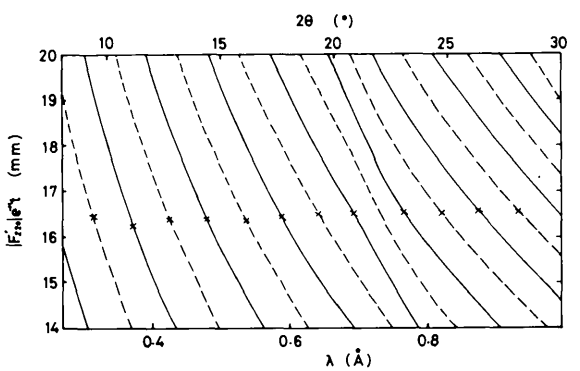

Fig. 7. Calculated maximum (solid line) and minimum (broken line) positions in the *Pendellösung* beat for the 220 reflection. The measured points in Fig. 6 for specimen 2 are plotted on the lines (×).

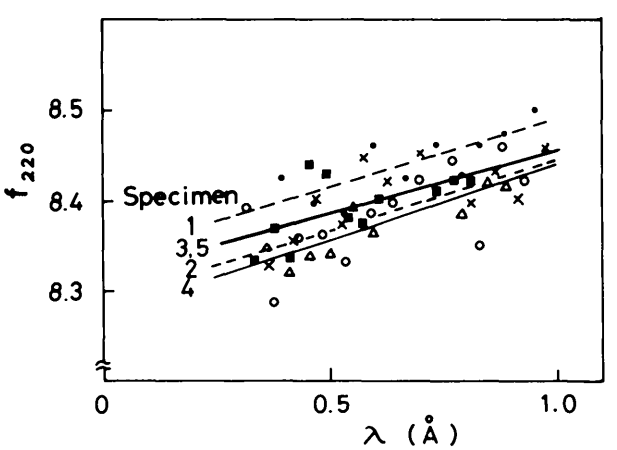

Fig. 8. Variations in f_{220} with λ. Values obtained for five specimens with different thicknesses are plotted together. Lines are drawn by the least-squares method. ● Specimen no. 1, $t = 0{\cdot}195$ mm; ○ no. 2, $t = 0{\cdot}245$ mm; × no. 3, $t = 0{\cdot}249$ mm; △ no. 4, $t = 0{\cdot}289$ mm; ■ no. 5, $t = 0{\cdot}345$ mm.

change must be originated by f'. Cromer (1965) has calculated f' for elements nos. 10 through 98 by using relativistic Dirac–Slater wave functions. Cromer's values for silicon are shown in Fig. 9; they have been approximated in the present experimental range (0·3 Å $< \lambda <$ 1·0 Å) as a linear function of λ, *i.e.* $f' = 0{\cdot}16\,\lambda - 0{\cdot}03$.

The f_{hkl} values obtained in the present work for various reflections are represented as a linear function of λ in Table 1. The lines were drawn by using the least-squares method as shown in Fig. 9. It should be stated that the obtained values of the gradient were roughly the same as Cromer's value, 0·16, except for higher-index reflections. The f_{hkl} values at $\lambda = 0{\cdot}5594$ Å (Ag $K\alpha_1$) are also given in Table 1 to allow a comparison with the previous values so far obtained by using characteristic X-rays.

4. Discussion

The advantage of the present method is that one can measure the wavelength λ of diffracted X-rays simultaneously with the intensity measurement. The intensity variation with λ can be obtained directly by the detector with a counting device and not indirectly as in the photographic method. This technique only requires the sample to have an equal thickness over the irradiated area, which was about 1 mm in diameter in the present experiment. One gets various reflections from the same small region of the specimen without any shaping procedure as shown in Fig. 9. It is worth noting that this technique not only makes the measurement for silicon or germanium easy but also makes the experiment possible for materials for which it is difficult to grow large single crystals without lattice defects.

The solid line in Fig. 5 indicates the calculated J_{220}/I_0 from (1) by using $f_{220} = 8{\cdot}29 + 0{\cdot}15\,\lambda$ with Cromer's f'' values and the Victoreen equation for μ. One can see in the figure that the agreement between the calculated and observed intensity beat is fairly good. In the above calculation the area under the profile has been normalized for both cases. A slight discrepancy between the solid line and the dots with respect to the ordinate value is supposed to be due to the error in measuring $I_0(E)$.

In the case where the incident beam is unpolarized, the diffracted intensity oscillates with two periods, *i.e.* with A_n and A_p in (3): the two beats may be superimposed to produce a fade-out phenomenon which has been called 'fading'. For large values of $A_{n,p}$, as in the present experiment, the oscillations are of sinusoidal nature with period $\Delta A_{n,p} = \pi$. Accordingly, the fading region of nth order appears at the position where the following relation holds:

$$A_n - A_p = (e^2/mc^2)(\lambda t/\cos\theta)|F'_{hkl}|e^{-M}(1 - |\cos 2\theta|)/V = (2n-1)\pi/2 \quad (n = \text{integer}).$$

For example, for the 220 reflection, the fading region of first order appears at about $2\theta = 22°$ when the specimen thickness is 0·245 mm. The measured fading region agrees very well with the calculation as shown in Fig. 5.

The extremum positions in the intensity beat as shown in Fig. 6 can be determined with errors which depend on the amount of total integrated intensity for the measured points. Accordingly, the peak positions at lower angles, for example $12 < 2\theta < 20°$ in Fig. 3, can be determined more accurately than those at higher angles ($25° < 2\theta$). However, as one sees from the gradient of lines in Fig. 7, the values of $|F'_{hkl}|e^{-M}t$ corresponding to the extremum positions will be

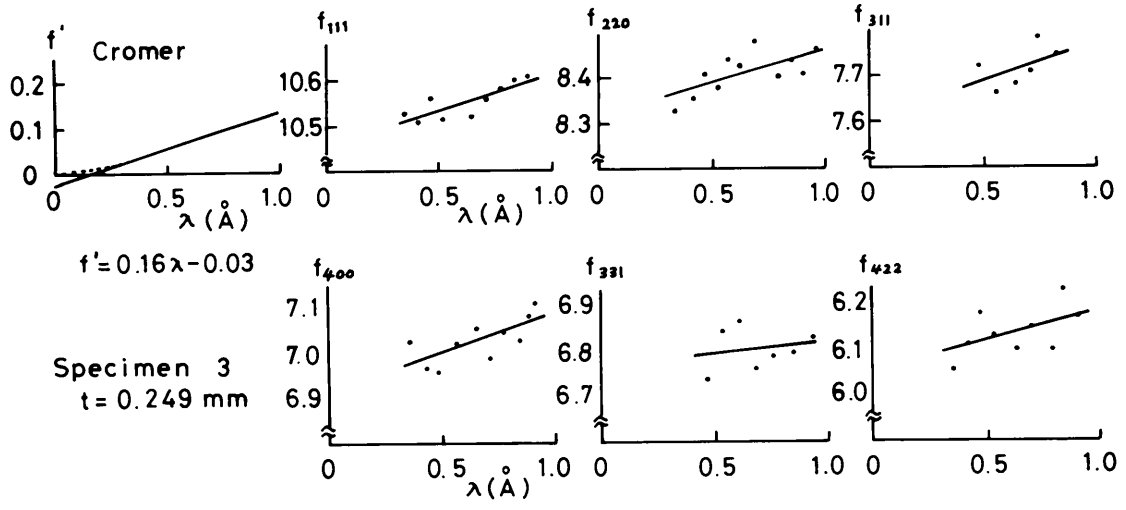

Fig. 9. Wavelength dependence of f_{hkl} for various reflections. A linear dependence on λ is assumed in the experimental range. The calculated dependence of the dispersion correction term f' by Cromer (1965) is also shown.

determined with a higher accuracy at higher 2θ values. So the errors in $|F'_{hkl}|e^{-M}t$ will roughly be equal in the whole range, for example $10 < 2\theta < 30°$, of diffraction angle or of wavelength λ except in the fading region.

The thickness of the specimen was measured by a micrometer with the minimum vernier scale of 1 μm. The fractional error in the thickness measurement is $3–5 \times 10^{-3}$. Moreover, because of the nature of thickness measurement with a micrometer, only the thick part of the specimen may be measured if it has non-uniform thickness. Consequently, it is possible to obtain smaller values of the structure factor. The error involved in the f_{hkl} values can be estimated from Fig. 8 or Fig. 9. Even though the individual f_{hkl} value at one λ contains rather large errors depending on the intensities of the *hkl* reflections, the lines of f_{hkl} with respect to λ can be drawn with smaller errors, as shown in Table 1. The lines drawn in Fig. 8 show the wavelength dependence of f_{220} corresponding to the five specimens with different thicknesses. From the scattering of the measured points around the lines one might recognize that the error in the thickness measurement is rather noticeable.

In the present study the incident radiation is assumed to be unpolarized. However, as Slivinsky (1971) has reported, white radiation emitted by commericial X-ray tubes with thick targets is usually polarized depending upon the photon energy and applied voltage. Olsen, Buras, Jensen, Alstrup, Gerward & Selsmark (1978) have recently made a quantitative measurement of polarization for copper and tungsten tubes and present a diagram showing the amount of polarization as a function of the ratio of photon energy to incident electron energy. We checked the effect of polarization on the present experimental data in the structure-factor determination using the above diagram of Olsen *et al.* (1978). The polarization, defined by the intensity ratio between the difference and sum of the normal and parallel components, was about 5% in the present experiment. A calculation showed that the shift of extremum positions in Fig. 7 due to the polarization was rather remarkable in the fading region. Nevertheless, the effect of polarization on the measured values of the structure factor was 0·3% at the most.

It is concluded from this work that the observed atomic scattering factors of silicon show a clear wavelength dependence very close to that expected by Cromer's (1965) calculation for anomalous dispersion. As shown in Table 1, the averaged f_{hkl} values at $\lambda =$ 0·5594 Å (Ag $K\alpha_1$) are a little smaller than the values of Hattori *et al.* (1965) over a wide range of $\sin\theta/\lambda$ except for the 400 reflection. The values for the 111 and 220 reflections in this work were close to those measured by Tanemura & Kato (1972) using interferometry fringes.

The authors are greatly indebted to Professor N. Kato of Nagoya University for his valuable comments on the manuscript. They also greatly acknowledge Dr T. Abe of Shin-Etsu Semiconductor Company for kindly supplying perfect silicon single crystals.

References

ARISTOV, V. V., SHMYTKO, I. M. & SHULAKOV, E. V. (1977*a*). *Acta Cryst.* A**33**, 412–418.

ARISTOV, V. V., SHMYTKO, I. M. & SHULAKOV, E. V. (1977*b*). *Acta Cryst.* A**33**, 418–423.

BATTERMAN, B. W. & PATEL, J. R. (1968). *J. Appl. Phys.* **39**, 1882–1887.

BURAS, B., OLSEN, J. S., GERWARD, L., SELSMARK, B. & LINDEGAARD ANDERSEN, A. (1975). *Acta Cryst.* A**31**, 327–333.

CROMER, D. T. (1965). *Acta Cryst.* **18**, 17–23.

DEMARCO, J. J. & WEISS, R. J. (1965). *Acta Cryst.* **19**, 68–72.

HART, M. (1966). *Z. Phys.* **189**, 269–291.

HART, M. & MILNE, A. D. (1969). *Acta Cryst.* A**25**, 134–138.

HASHIMOTO, H. (1965). *Appl. Phys. Lett.* **6**, 16–17.

HATTORI, H., KURIYAMA, H., KATAGAWA, T. & KATO, N. (1965). *J. Phys. Soc. Jpn*, **20**, 988–996.

International Tables for X-ray Crystallography (1962). Vol. III. Birmingham: Kynoch Press.

JAMES, R. W. (1967). *The Optical Principles of the Diffraction of X-rays*. London: G. Bell and Sons.

KATO, N. (1955). *J. Phys. Soc. Jpn*, **10**, 46–55.

KATO, N. & LANG, A. R. (1959). *Acta Cryst.* **12**, 787–794.

KOZAKI, S., OHKAWA, T. & HASHIMOTO, H. (1968). *J. Appl. Phys.* **39**, 3967–3976.

OLSEN, J. S., BURAS, B., JENSEN, T., ALSTRUP, O., GERWARD, L. & SELSMARK, B. (1978). *Acta Cryst.* A**34**, 84–87.

PERSSON, E., ZIELIŃSKA-ROHOZIŃSKA, E. & GERWARD, L. (1970). *Acta Cryst.* A**26**, 514–518.

SLIVINSKY, V. W. (1971). *Bull. Am. Phys. Soc.* **16**, 546 (abstract only).

TANEMURA, S. & KATO, N. (1972). *Acta Cryst.* A**28**, 69–80.

YAMAMOTO, K., HOMMA, S. & KATO, N. (1968). *Acta Cryst.* A**24**, 232–237.

YASUDA, Y., HONDOH, T. & HIGASHI, A. (1979). *Jpn. J. Appl. Phys.* **18**, 1845–1846.